



Novel fluorosilicone triblock copolymers prepared by two-step RAFT polymerization: Synthesis, characterization, and surface properties

Cheng-Mei Guan, Zheng-Hong Luo *, Jing-Jing Qiu, Pei-Ping Tang

Department of Chemical and Biochemical Engineering, College of Chemistry and Chemical Engineering, Xiamen University, Xiamen 361005, People's Republic of China

ARTICLE INFO

Article history:

Received 24 February 2010

Received in revised form 26 March 2010

Accepted 7 April 2010

Available online 10 April 2010

Keywords:

Triblock copolymers

PDMS-*b*-PHFBMA-*b*-PS

RAFT polymerization

Microphase-separated structure

Controlled manner

ABSTRACT

Well-defined poly(dimethylsiloxane)-*b*-poly(2,2,3,3,4,4,4-heptafluorobutyl methacrylate)-*b*-poly(styrene) (PDMS-*b*-PHFBMA-*b*-PS) triblock copolymers were prepared by two-step reversible addition-fragmentation chain transfer (RAFT) polymerization. The two-step RAFT polymerization proceeded in a controlled manner as demonstrated by the macromolecular characteristics of the blocks and corresponding polymerization kinetic data. Furthermore, surface properties and morphologies of the polymers were investigated with static water contact angle (WCA) measurement, X-ray photoelectron spectroscopy (XPS), transmission electron microscopy (TEM) and atomic force microscopy (AFM) which showed low surface energy and microphase-separation surfaces.

© 2010 Elsevier Ltd. All rights reserved.

1. Introduction

Recently, increasing attention has been attracted to the combined incorporation of siloxane moieties and fluorinated groups into synthetic materials. The comprehensive properties of these materials, which combines advantages of both siloxane and fluorinated polymers, are excellent, including weather resistance, low surface energy, chemical resistance, etc. [1–5] They have been widely used as surface modification agents for improving surface properties in the fields of coatings, adhesives, films, fibers and moldings, etc. [4–7]. Various fluorosilicone block copolymers containing poly(dimethyl-siloxane) (PDMS) and fluorocarbon segments have previously been prepared in our laboratory [5,8,9]. The synthesis and applications of fluorosilicone block copolymers have also been reviewed [10,11], and several methods of preparation of fluorosilicone block copolymers have been reported. For instance, Kim et al. [12–14] reported the fluorosilicone block copolymers of poly(perfluoroalkylethyl acrylate)-*b*-poly(3-[tris(trimethylsilyloxy)-

silyl] propyl methacrylates) (PFA-*b*-PSiMAs) prepared by a three-step synthetic approach. In the first step, the free-radical polymerization was applied to prepare PFA macromonomer (PFAM). Then, PFAM initiator (PFAMI) was prepared via the condensation reaction. At last, the reaction of PFAMI and SiMA was used to prepare the PFA-*b*-PSiMAs block copolymers. Recently, Boutevin et al. [15–17] reported the synthesis of the fluorosilicone block copolymers. However, Boutevin et al. [15] prepared the photocrosslinkable fluorinated PDMS via two-step hydrosilylation. More recently, Luo et al. [5,8,9] prepared the fluorosilicone block copolymers of PDMS-*b*-poly(methyl methacrylate)-*b*-poly(2,2,3,3,4,4,4-heptafluorobutylmethacrylate) (PDMS-*b*-PMMA-*b*-PHFBMA) and PDMS-*b*-PHFBMA via atom transfer radical polymerization (ATRP). Based on above discussion, it becomes clear that the fluorosilicone block copolymers have been achieved mainly by living anionic polymerization and ATRP. No detailed research has been done using the RAFT technique to prepare them. In this article, we investigate the synthesis of poly(dimethylsiloxane, DMS)-*b*-poly(2,2,3,3,4,4,4-heptafluorobutyl methacrylate, HFBMA)-*b*-poly-(styrene, St) (PDMS-*b*-PHFBMA-*b*-PS) in a two-step RAFT polymerization, which starts from the RAFT polymerization of HFBMA and ends in RAFT of St.

* Corresponding author. Tel.: +86 592 2187190; fax: +86 592 2187231.
E-mail address: luozh@xmu.edu.cn (Z.-H. Luo).

Obviously, during this last decade the RAFT polymerization has already been used to prepare siloxane polymers or fluorinated polymers, along with homo- and copolymerizations of siloxane/fluorinated methacrylates and acrylates, and siloxane/(fluorinated) St, alone or in combination with other monomers [10,11,18–25]. Unfortunately, the chain transfer ability of xanthates (usually used as the chain transfer agent of RAFT polymerization of St) was poor, resulting in polydispersities (PDIs) of polymers ranging from 1.5 to 2 in the past [18,25]. However, up to now, the synthesis of fluorinated polysiloxanes through the RAFT polymerization was not described. Thus, we were interested in studying the application of this method in the synthesis of fluorinated polysiloxanes in order to develop a novel approach to synthesize fluorosilicone copolymers.

It was interesting to test the structures and surface properties of the newly synthesized fluorosilicone block copolymers. For this purpose, we used a PDMS-macro-RAFT agent to mediate polymerization of methacrylate monomers with fluorinated side groups to prepare fluorosilicone triblock polymers. To get triblock copolymers with low surface energy, we designed novel PDMS-*b*-PHFBMA-*b*-PS triblock copolymers. Therefore, a novel approach to synthesize fluorosilicone copolymers and novel fluorosilicone triblock copolymers are helpful to the further study in the controlled/living radical polymerization techniques applied in fluorosilicone polymers.

2. Experimental

2.1. Materials

Monohydroxyl-terminated polydimethylsiloxane (PDMS-OH, 5000 g/mol determined by GPC) and 2-bromoisobutrylbromide (98%) were obtained from A Better Choice for Research Chemicals GmbH & Co. KG. Triethylamine (99%) was supplied by Sinopharm Chemical Reagent Co, Ltd. (SCRC) and stored with 4-Å molecular sieves. Styrene (St) obtained from Guangdong Xilong Chemical Co, Ltd. was rinsed with 5 wt.% aqueous NaOH solution to remove the inhibitor. 2,2,3,3,4,4,4-heptafluorobutyl methacrylate (HFBMA, Lancaster, 98%) was also washed with 5 wt.% aqueous NaOH solution to remove inhibitor before polymerization. Azobisisobutyronitrile (AIBN) obtained from Shanghai No.4 Reagent & H.V. Chemical Co, Ltd. was recrystallized from ethanol. Potassium *O*-ethylxanthate was supplied by J&K Chemical Co, Ltd and used without further purification. All other reagents and solvents were obtained from SCRC and used without further purification.

2.2. Measurements

Proton nuclear magnetic resonance (^1H NMR) was performed on a Bruker AV400 instrument with deuterated chloroform as the solvent. Fourier transform infrared (FT-IR) spectra were obtained on an Avatar 360 FT-IR spectrophotometer. Gel permeation chromatography (GPC) was carried out using tetrahydrofuran (THF) at a flow rate of 1 ml/min, with a Waters 1515 isocratic HPLC pump

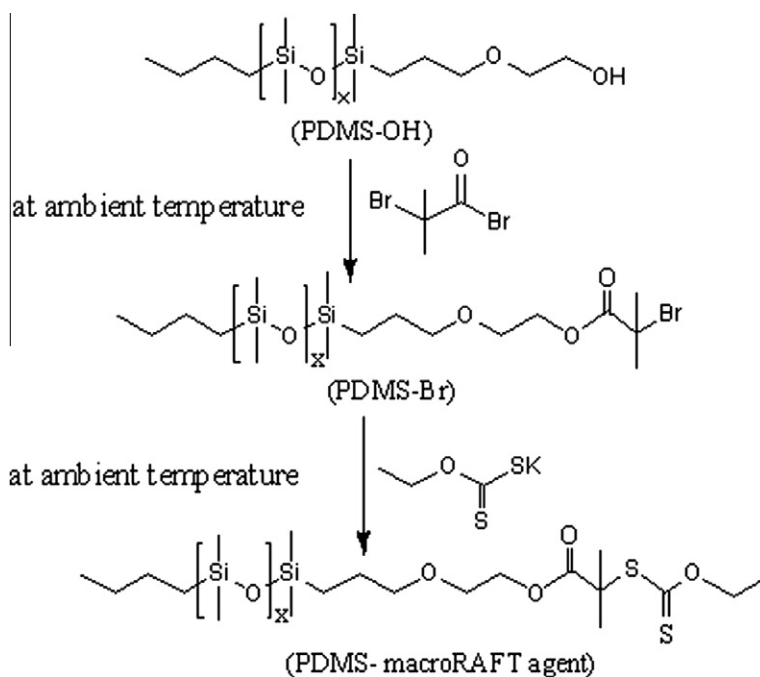
equipped with a Waters 2414 refractive index detector and three Waters Styragel HR columns (1×104 , 1×103 , and 500 Å pore sizes). Monodisperse polystyrene standards were used for calibration. Static water contact angles of the diblock and triblock copolymer films were measured on a telescopic goniometer (SL-200B). For each angle reported, at least seven sample readings from different surface locations were averaged. The morphologies of the PDMS-*b*-PHFBMA-*b*-PS triblock copolymers were identified by transmission electron microscopy (TEM). The thin film was obtained via the slow evaporation technique: 25 ml THF was poured into a dry and sealed desiccator to form a solvent atmosphere. A drop of 1 wt.% polymer solution was applied onto a copper grid coated with carbon, and then the grid was placed in the desiccator for 72 h to eliminate trace solvent. A transmission electron microscope (TecnaiF30) was used with an accelerating voltage of 300 kV. Besides, Atomic force microscopy (AFM) images were observed on NanoScope SPM (Veeco, USA) in ultra-light-tapping mode under ambient conditions (25 °C, 40% RH). X-ray photoelectron spectroscopy (XPS) spectra were recorded with a PHI quantum 2000 scanning ESCA microprobe, equipped with an Al $K\alpha_{1,2}$ monochromatic source of 1486.60 eV. The beam was 200 μm in diameter and the analysis area was $1.5 \times 0.2 \text{ mm}$. The measurements were typically operated at 35 W. A typical multiplex pass energy was 29.35 eV, and a typical survey pass energy was 187.85 eV. XPS samples were made as follows: the block copolymers were dissolved in THF, then cast onto aluminum foil, and dried in vacuum at room temperature.

2.3. Synthesis of bromine end-capped PDMS (PDMS-Br)

Synthesis of PDMS-Br via the esterification reaction of 2-bromoisobutrylbromide with a commercially available PDMS-OH (Scheme 1) has been described previously [8,26,27]. The product is pale yellow oil (yield: 4.1712 g, 85%) and used for the preparation of PDMS-macro-RAFT agent. ^1H NMR (δ , ppm, in CDCl_3): 0.1 (m, 396H, $-\text{Si}(\text{CH}_3)_2$), 0.55 (m, 4H, $-\text{SiCH}_2$), 0.90 (m, 3H, $-\text{CH}_3$), 1.33 (m, 4H, $-\text{CH}_2$), 1.58 (m, 2H, $-\text{CH}_2\text{CH}_2\text{O}$), 1.96 (s, 6H, $-\text{C}(\text{CH}_3)_2\text{Br}$), 3.46 (t, 2H, $-\text{CH}_2\text{O}$), 3.70 (t, 2H, $-\text{OCH}_2$), 4.34 (t, 2H, $-\text{CH}_2\text{OCO}$). FT-IR (liquid): 2964 cm^{-1} (alkyl C–H stretching), 1742 cm^{-1} ($-\text{C}=\text{O}$ stretching), 1260 cm^{-1} ($-\text{Si}(\text{CH}_3)_2$ flexing) and 1000–1100 cm^{-1} (Si–O stretching).

2.4. Synthesis of xanthate-capped PDMS (PDMS-macro-RAFT agent)

We prepared xanthate-capped PDMS as the PDMS-macro-RAFT agent (the detailed experimental procedures are described in Appendix A). ^1H NMR (δ , ppm, in CDCl_3): 0.1 (m, 396H, $-\text{Si}(\text{CH}_3)_2$), 0.55 (m, 4H, $-\text{SiCH}_2$), 0.90 (m, 3H, $-\text{CH}_3$), 1.33 (m, 4H, $-\text{CH}_2$), 1.45 (s, 3H, $-\text{OCH}_2\text{CH}_3$), 1.58 (m, 2H, $-\text{CH}_2\text{CH}_2\text{O}$), 1.96 (s, 6H, $-\text{C}(\text{CH}_3)_2\text{Br}$), 3.46 (t, 2H, $-\text{CH}_2\text{O}$), 3.70 (t, 4H, $-\text{OCH}_2$), 4.34 (t, 2H, $-\text{CH}_2\text{OCO}$). FT-IR (liquid): 2964 cm^{-1} (alkyl C–H stretching), 1742 cm^{-1} ($-\text{C}=\text{O}$ stretching), 1260 cm^{-1} ($-\text{Si}(\text{CH}_3)_2$ flexing) and 1000–1100 cm^{-1} (Si–O stretching).



Scheme 1. Synthetic Scheme of the PDMS-macroRAFT agent.

2.5. Synthesis of PDMS-*b*-PHFBMA diblock copolymers

The RAFT polymerization was carried out in a dry flask surrounded by the inert atmosphere of nitrogen. The polymerization of HFBMA using AIBN as initiator proceeded with initial molar ratio of each component of $[M]/[\text{RAFT agent}]/[I] = 50:1:1$ (Scheme 2). AIBN (0.0146 g, 0.0890 mmol) and PDMS-macroRAFT agent (0.4622 g, 0.0890 mmol) were charged into a dry two-neck flask along with a magnetic stirrer bar. Vacuum was then applied (pumped) and the flask was flushed with nitrogen, which was repeated for three times. HFBMA (0.887 ml, 4.45 mmol) and toluene (1.210 ml) were added to the flask using degassed syringes. The solution was flushed with nitrogen as described above, and then heated to 60 °C in oil bath. Samples were taken periodically with a syringe. The reaction was stopped after 4 h. The reaction mixtures were diluted with THF, and precipitated in methanol. The obtained polymer was rinsed with methanol for several times and dried to constant weight under vacuum at 50 °C (yield: 1.4023 g, 84%). The overall monomer conversion rate was determined gravimetrically.

2.6. Synthesis of PDMS-*b*-PHFBMA-*b*-PS triblock copolymers

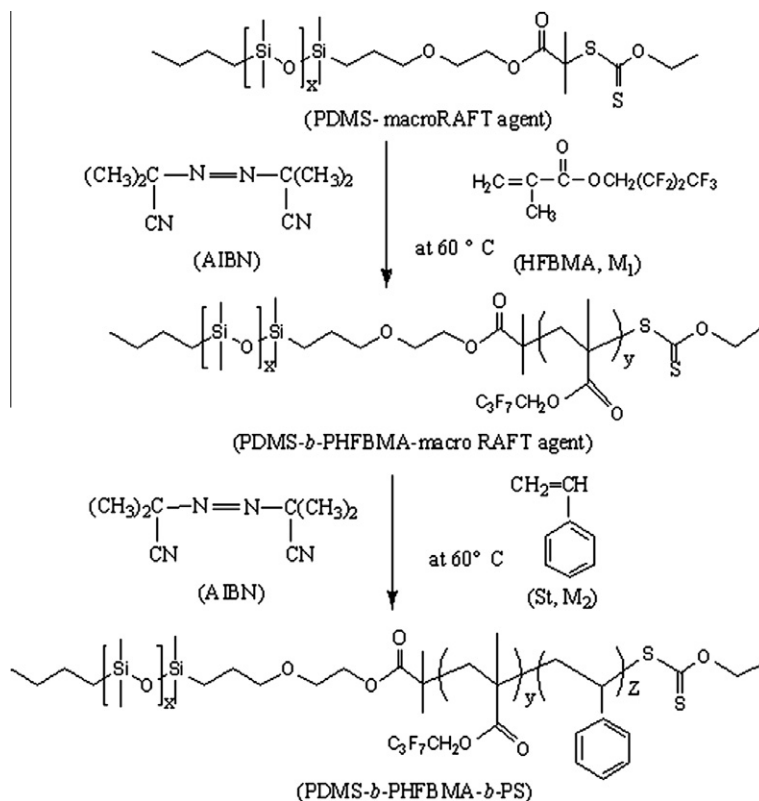
As PDMS-*b*-PHFBMA diblock copolymers synthesized above are xanthate-capped, therefore, they can act as macroRAFT agent to further synthesize triblock copolymers. The polymerization of St using AIBN as initiator proceeded with initial molar ratio of each component of $[M]/[\text{RAFT agent}]/[I] = 100:1:1$ (Scheme 2). AIBN (0.0064 g, 0.0390 mmol) and PDMS-macroRAFT agent (0.6248 g, 0.0390 mmol) were charged into a dry two-neck flask

along with a magnetic stirrer bar. Vacuum was then pumped and the flask was flushed with nitrogen, which was repeated for three times. St (0.448 ml, 3.90 mmol) and toluene (1.100 ml) were added to the flask using degassed syringes. The solution was flushed with nitrogen as described above, and then heated to 60 °C in an oil bath. Samples were taken periodically with a syringe. The reaction was stopped after 5 h. The reaction mixtures were diluted with THF, and precipitated in methanol. The obtained polymer was rinsed with methanol for several times and dried to constant weight under vacuum at 50 °C (yield: 0.8916 g, 86%). The overall monomer conversion rate was determined gravimetrically.

3. Results and discussion

3.1. Synthesis of bromine end-capped PDMS (PDMS-Br)

Taking into considerations of the appropriate molecular weight and end group structures, we choose PDMS. The reaction was completed with a high yield and the chemical structure of the resulting product was fully characterized prior to polymerization by ^1H NMR and FT-IR (Supplementary characterization data (by ^1H NMR and FT-IR) of product are given in Appendix B). The sharp singlet at 1.96 ppm in the ^1H NMR corresponds to the two methyl groups α to the bromide atom. The chemical shift of 4.34 ppm belongs to monocarbinol-terminated PDMS-OH that has been converted to bromine end-capped PDMS (PDMS-Br). The PDMS-Br has a distinctive peak in the ^1H NMR spectrum, assigned to the dimethylsiloxane repeat units, at 0.1 ppm. Integral ratio of the dimethylsiloxane repeat units to the region at 4.34 ppm can be used to calculate absolute M_n value. The IR absorption at 1740 cm^{-1} is ascribed to the



Scheme 2. Synthetic Scheme of the PDMS-*b*-PHFBMA-*b*-PS triblock copolymers.

ester group, suggesting that the bromine end-capped PDMS (PDMS-Br) was successfully synthesized.

3.2. Synthesis of xanthate-capped PDMS (PDMS-macro-RAFT agent)

The RAFT polymerization is accomplished by performing a radical polymerization in the presence of certain compounds which all act as reversible chain transfer agents (including dithioesters, dithiocarbamates, trithiocarbonates, and xanthates) [29–32]. Few RAFT agents are commercially available. Accordingly, it is necessary to synthesize a suitable agent before polymerization in our present work. The attachment of a RAFT agent to a compound via functional groups has been employed for the synthesis of complex polymer architectures. Hydroxyl terminated PDMS allows the coupling of a RAFT agent via ester formation on both chain ends, resulting in polymeric RAFT agents suitable for the preparation of block copolymers. In our present work, The PDMS-macro-RAFT agent with a xanthate group was prepared for RAFT polymerization to form one block of the copolymers. The structure of the resulting macro-RAFT agent is similar to that of xanthates with a longer chain, which can be used to mediate RAFT polymerization. The final macro-RAFT agent was also characterized by ^1H NMR and FT-IR (Supplementary characterization data (by ^1H NMR and FT-IR) of product are also given in Appendix B). In the ^1H NMR spectrum, there is a peak at 1.45 ppm and it is assigned to the methyl group

next to $-\text{OCH}_2$ group, indicating that the PDMS-macro-RAFT agent with xanthate group has been successfully synthesized. The FT-IR peaks of the $-\text{C}=\text{S}$ and $-\text{C}-\text{S}$ group at $1020\text{--}1065\text{ cm}^{-1}$ and $1000\text{--}1054\text{ cm}^{-1}$ are overlapped with peaks at $1000\text{--}1100\text{ cm}^{-1}$ that correspond to the characteristic peaks of the $(-\text{Si}(\text{CH}_3)_2)$ group, which also demonstrates that the macro-RAFT agent has been achieved. The molecular weight calculated from MS agrees with the theoretical value.

3.3. Synthesis of PDMS-*b*-PHFBMA diblock copolymers

Well-defined PDMS-*b*-PHFBMA diblock copolymers were prepared by the RAFT polymerization. Oxygen has significant influence on the RAFT polymerization, such as inhibiting polymerization and terminating radicals. Therefore, the system must be strictly deoxygenated before polymerization. The polymerization was carried out with the initial molar ratio of each component of $[\text{M}]/[\text{RAFT agent}]/[\text{I}] = 50:1:1$, giving a theoretical absolute M_n of approximately 18,590 g/mol with 100% conversion. After the PDMS-*b*-PHFBMA diblock copolymers were purified, their chemical structures were measured by ^1H NMR and FT-IR (Supplementary characterization data (by ^1H NMR and FT-IR) of product are given in Appendix B). The PDMS-*b*-PHFBMA diblock copolymers have two distinct peaks shown in the ^1H NMR spectrum, with one at 4.34 ppm corresponding to the hydrogen in the $-\text{OCH}_2(\text{CF}_2)_2\text{CF}_3$ group affected by both the ester group

and the $-\text{CF}_2$ group, and the other at 0.1 ppm representing PDMS moiety. Integral ratios of the two regions can be used to calculate the absolute M_n values of the diblock copolymers. The FT-IR spectrum of the PDMS-*b*-PHFBMA shown in Appendix B also proves that the PDMS polymers have distinctive peaks, centered between 1000 and 1100 cm^{-1} , corresponding to the $-\text{Si}-\text{O}$ group, while peaks at 1260 cm^{-1} are attributed to the $-\text{Si}(\text{CH}_3)_2$ group. Two peaks, centered at 1228 and 1182 cm^{-1} , are assigned to the anti-symmetric and symmetric stretching vibrations of the $-\text{CF}_3$ group, respectively. There are two medium bands at 563 and 726 cm^{-1} , corresponding to a combination of the cocking and wagging vibrations of the $-\text{CF}_2$ group. Monomer conversion was measured by gravimetry by drying the sampled PDMS-*b*-PHFBMA solution to constant weight in vacuum at 50 °C. Fig. 1a shows the kinetics plot for the polymerization of HFBMA. The linearity of the plot suggests first-order kinetics. Fig. 2a shows plot of M_n as a function of conversion for the polymerization of HFBMA. The plot provides excellent linearity, indicative of living polymerization, and the molecular weights determined by ^1H NMR are close to those predicted. The linearity of Figs. 1a and 2a strongly implies that the polymerization of HFBMA proceeds in a living manner. GPC was used to study the molecular weights and molar weight distributions of the resulting copolymers. GPC traces of the PDMS-macro-RAFT agent and PDMS-*b*-PHFBMA diblock copolymers are displayed in Fig. 3. For the sample examined, the molecular weight is 16,620 g/mol and the polydispersity (PDI) is 1.72. Generally, the chain transfer ability of xanthates is poor, leading to the PDI range of polymers from 1.5 to 2 [28,33–36]. We obtained the PDI of 1.72. This point would also be discussed in the next section. In addition, the molecular weights determined by ^1H NMR (15,910 g/mol (Appendix B) and GPC agree with the theoretically predicted ones.

3.4. Synthesis of PDMS-*b*-PHFBMA-*b*-PS triblock copolymers

The polymerization was carried out with the initial molar ratio of each component of $[\text{M}]/[\text{RAFT agent}]$

$[\text{I}]/[\text{M}] = 100:1:1$, giving a theoretical absolute M_n of approximately 26,310 g/mol with 100% conversion. The final PDMS-*b*-PHFBMA-*b*-PS block copolymers were characterized by ^1H NMR and FT-IR spectroscopy (Supplementary characterization data (by ^1H NMR and FT-IR) of product are given in Appendix B). In the ^1H NMR spectrum, the $-\text{Si}(\text{CH}_3)_2$ repeating units of PDMS segment, the $-\text{OCH}_2(\text{CF}_2)_2\text{CF}_3$ group of PHFBMA block, and the $-\text{OC}_6\text{H}_5$ group of PS block, produce the three characteristic peaks, centered at 0.1, 4.34, and 6.5–7.16 ppm, respectively. In the FT-IR spectrum, the characteristic peaks of the PDMS block appear between 1000 and 1100 cm^{-1} . The adsorption peak at 1742 cm^{-1} is attributed to stretching vibrations of the $\text{C}=\text{O}$ group of the PHFBMA segment. The characteristic peaks of the PS block appear at 700, 760, 1600, 3000–3100 cm^{-1} . Monomer conversion was measured by gravimetry by drying the sampled PDMS-*b*-PHFBMA-*b*-PS solution to constant weight in vacuum at 50 °C. Fig. 1b shows the kinetics plot for the polymerization of St. The linearity of the plot suggests first-order kinetics. Fig. 6b shows plot of M_n as a function of conversion for the polymerization of St. The plot provides excellent linearity, indicative of living polymerization, and the molecular weights determined by ^1H NMR are close to those predicted. The linearity of Figs. 1b and 2b strongly implies that the polymerization of St proceeds in a living manner. As a whole, the linearity of Figs. 1 and 2 implies that the polymerizations of HFBMA, (and) St both proceed in living manners. GPC was used to study the molecular weights and molar weight distributions of the synthesized copolymers. GPC traces of the PDMS-*b*-PHFBMA-*b*-PS triblock copolymers are displayed in Fig. 3. For the sample examined, the molecular weight is 26,280 g/mol and the PDI is 1.86. As described above, generally, the chain transfer ability of xanthate is not good and this causes the PDIs of polymers ranging from 1.5 to 2 [28,33–39]. Here, the obtained PDI value is within the range in our study. One knows that the general formula of xanthate is $\text{R}-\text{S}(\text{C}=\text{S})\text{OZ}$, where R and Z are both substitutional groups [28,33–39]. During the polymerization, the chain transfer ability of xanthate is influenced by R and Z. Researchers at first thought that

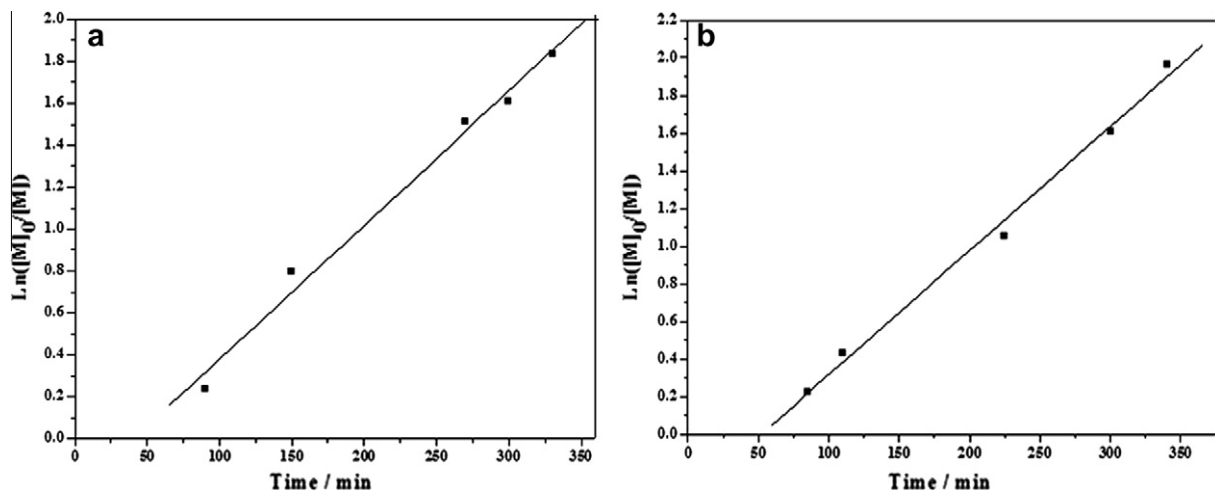


Fig. 1. First-order kinetic plot ((a) the RAFT polymerization of HFBMA, (b) the RAFT polymerization of St).

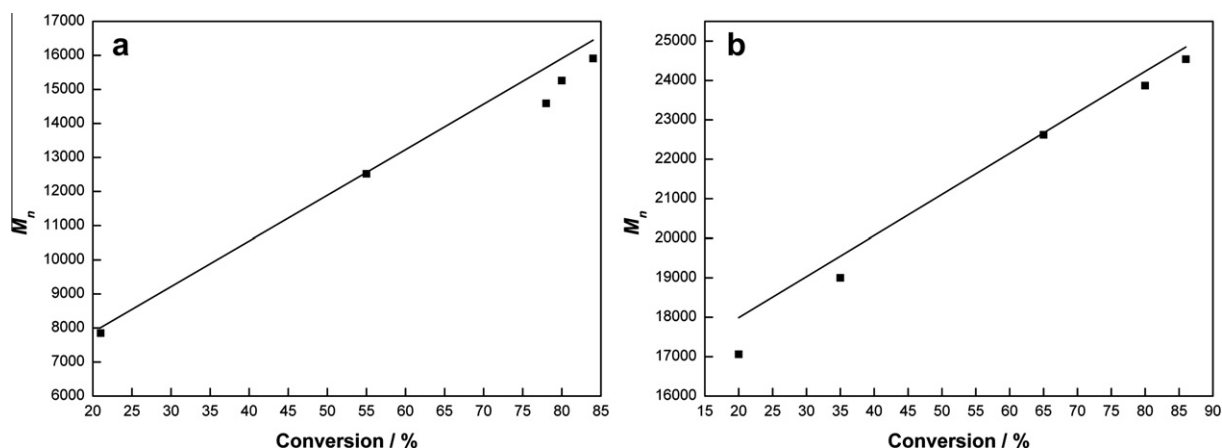


Fig. 2. Dependence of M_n of block polymers on the monomer conversion ((a) the RAFT polymerization of HFBMA, (b) the RAFT polymerization of St. The solid lines are corresponding theoretical lines.).

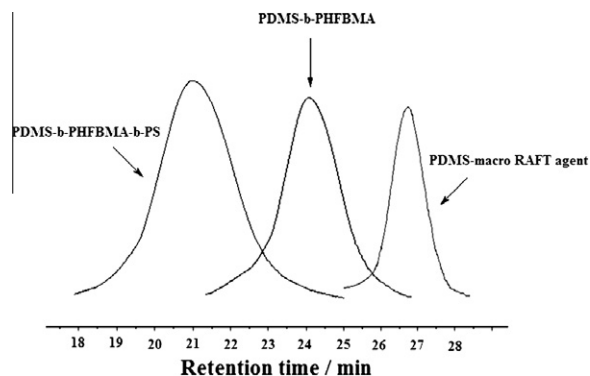


Fig. 3. GPC traces for PDMS-*b*-PHFBMA-*b*-PS (sample: DMS₆₅HFBMA₄₀St₈₃, $M_n = 25,280$, $M_w/M_n = 1.86$) prepared from PDMS-*b*-PHFBMA (sample: DMS₆₅HFBMA₄₀, $M_n = 16,620$, $M_w/M_n = 1.72$), PDMS-macro-RAFT agent ($M_n = 5720$, $M_w/M_n = 1.06$).

xanthate could not be used as the chain transfer reagent for the RAFT polymerization of St due to the excessively small chain transfer constant [28,37,38]. However, such a chain transfer function could be achieved by changing the structures of R and Z. One can also find that the design technique of R and Z is based on their stability and steric-conjugate electron-effect [28,35–39]. Namely, in this study, the successful RAFT polymerization of HFBM and St depends on appropriate R and Z and we made it. In practice, the PDI data above have proved this point. The molecular weights determined by ^1H NMR (24,540 g/mol (Appendix B)) and GPC are in agreement with the theoretically predicted ones. Moreover, the important polymerization data are shown in Tables 1 and 2.

3.5. Contact angles and surface energies of the copolymers

The contact angles and surface energies of the PDMS-*b*-PHFBMA diblock copolymers and PDMS-*b*-PHFBMA-*b*-PS triblock copolymers were investigated through WCA measurements. The results of the WCAs and surface ener-

Table 1

The RAFT Data for the polymerization of HFBMA at 60 °C.

Samples	DMS _x HFBMA _y	$M_{n,theo}^a$	$M_{n,NMR}^b$	Conv ^c (%)	PDI ^d
No. 1	DMS ₆₅ HFBMA _{9.9}	8010	7850	21	1.78
No. 2	DMS ₆₅ HFBMA _{27.3}	12,560	12,520	55	1.63
No. 3	DMS ₆₅ HFBMA _{35.1}	15,640	14,590	78	1.68
No. 4	DMS ₆₅ HFBMA _{37.6}	15,910	15,260	80	1.76
No. 5	DMS ₆₅ HFBMA ₄₀	16,450	15,910	84	1.72

Where, a represents the theoretical molecular weight; b represents the molecular weight measured by ^1H NMR; c represents the monomer conversion data calculated by the gravimetry by drying sample to constant weight in a vacuum oven at 50 °C; d. obtained from GPC.

Table 2

The RAFT Data for the polymerization of St at 60 °C.

Samples	DMS _x HFBMA _y	$M_{n,theo}^a$	$M_{n,NMR}^b$	Conv ^c (%)	PDI ^d
No. 1	DMS ₆₅ HFBMA ₄₀ St _{11.1}	17,990	17,060	20	1.83
No. 2	DMS ₆₅ HFBMA ₄₀ St _{29.7}	19,550	19,000	35	1.69
No. 3	DMS ₆₅ HFBMA ₄₀ St _{64.5}	22,670	22,620	65	1.73
No. 4	DMS ₆₅ HFBMA ₄₀ St _{76.5}	24,230	23,870	80	1.76
No. 5	DMS ₆₅ HFBMA ₄₀ St ₈₃	24,850	24,540	86	1.86

Where, a represents the theoretical molecular weight; b represents the molecular weight measured by ^1H NMR; c represents the monomer conversion data calculated by the gravimetry by drying to constant weight in a vacuum oven at 50 °C; d. obtained from GPC.

gies are shown in Fig. 4. The WCAs toward the air-side surface of the PDMS-*b*-PHFBMA and PDMS-*b*-PHFBMA-*b*-PS films are about 107° (Fig. 4b) and 122° (Fig. 4c), respectively. Surface energies of the copolymers were indirectly obtained from WCAs. The equation of $1 + \cos \theta = 2(\gamma_s/\gamma_L)^{1/2} \exp[-\beta(\gamma_L - \gamma_s)]^2$, which was derived by Li and Neumann [40,41], is applied to calculate the surface energies. Where β is a constant with a value of 0.0001247 (m²/mJ)², determined from contact angle data for low energy solids. γ_s , γ_L , and θ are the surface energy of the solid, the surface energy of the test liquid, and the WCA, respectively. Therefore, we figure out that the surface energies of the

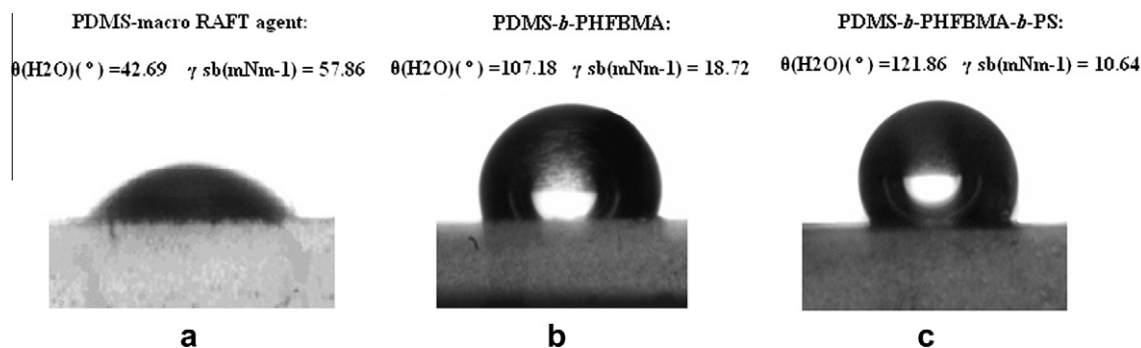


Fig. 4. Static WCA image ((a) PDMS-macro-RAFT agent, (b) DMS₆₅HFBMA₄₀, (c) DMS₆₅HFBMA₄₀St₈₃).

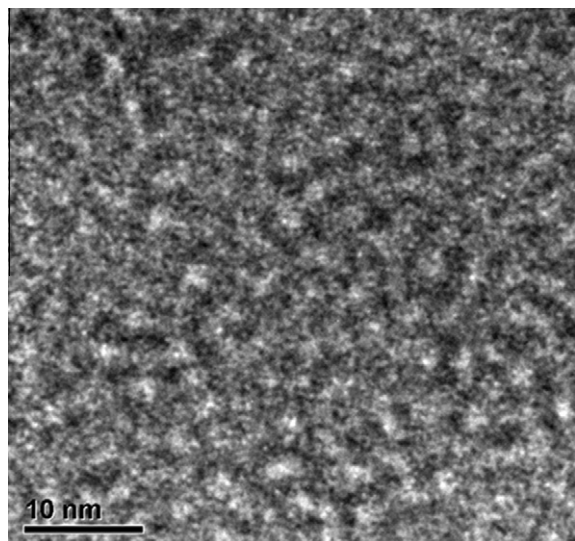


Fig. 5. TEM micrographs of the PDMS-*b*-PHFBMA-*b*-PS triblock copolymers.

PDMS-*b*-PHFBMA diblock copolymers and PDMS-*b*-PHFBMA-*b*-PS triblock copolymers are 18.72 and 10.64 mNm⁻¹, respectively. Compared with the PDMS-macro-RAFT agent (57.86 mNm⁻¹ shown in Fig. 4a), the surface energies of the PDMS-*b*-PHFBMA diblock copolymers and PDMS-*b*-PHFBMA-*b*-PS triblock copolymers are much lower. WCA measurements show that the PDMS-*b*-PHFBMA-*b*-PS triblock copolymer films are hydrophobic.

3.6. Microphase-separation behavior and surface compositions of the copolymers

Since surface microphase-separation has a great impact on the surface energy. The morphologies of the PDMS-*b*-PHFBMA-*b*-PS triblock copolymers were investigated with the help of TEM and AFM measurements. In the TEM bright-field pictures (Fig. 5) the PDMS-*b*-PHFBMA micro-domains appear black, while regions correspond to the PS block are bright. PS domains coagulate in the continuous PDMS-*b*-PHFBMA matrix, and some wormlike domains of PS appear with a length scale of about 3 nm and a periodicity of about 5 nm.

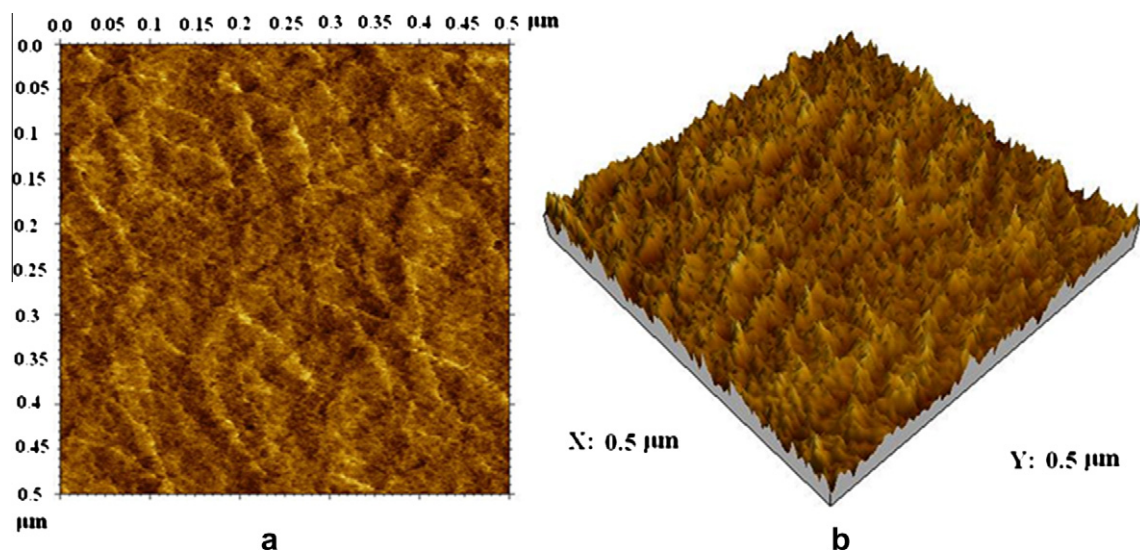


Fig. 6. AFM phase image and 3D image of DMS₆₅HFBMA₄₀St₈₃ ((a) AFM phase image, (b) 3D image).

Table 3

Surface compositions of fluorosilicone block copolymers measured by XPS.

Sample	F (in bulk) (%)	C 1s (%)	O 1s (%)	Si 2p (%)	F 1s (%)	F/Si
DMS ₆₅ HFBMA ₄₀	33.4	43.7	21.5	18.3	16.5	0.90
DMS ₆₅ HFBMA ₄₀ St ₈₃	21.7	39.8	18.9	12.7	28.6	2.25

Fig. 6 illustrates the typical AFM images of the PDMS-*b*-PHFBMA-*b*-PS copolymers, which are believed to be the result of the phase separation. Furthermore, according to the consistency between TEM and AFM, we confirm the attribution of two-phases in the AFM image. In AFM images the low spots appear as dark patches and the high spots as bright areas. Hydrophobic patches appear as low spots and less hydrophobic areas as high spots [9,42]. Therefore, the hydrophobic patches are dark in phase image and the hydrophilic areas are bright in the AFM topographical image obtained under ultra-light-tapping mode [43,44]. In Fig. 6a, dark patches are the hydrophobic PDMS-*b*-PHFBMA domains, and bright phases are the hydrophilic PS domains. The following data was obtained from the AFM software along with NanoScope SPM IIa. The average height of the protuberant area shown in Fig. 6b is 9.78 nm, the size of the distribution phase area is about 20–40 nm, and root mean square roughness in an area of 1000 × 1000 nm² of this sample is 1.52 nm. Surface microphase separation in the PDMS-*b*-PHFBMA-*b*-PS copolymers can be obtained. Moreover, the surface microphase separation in the PDMS-*b*-PHFBMA-*b*-PS copolymers can be determined by the surface chemical composition.

Surface composition was analyzed by XPS (Supplementary XPS data of diblock and triblock copolymer samples

are given in Appendix C). Their surface atomic contents of C 1s, O 1s, Si 2p, and F 1s are listed in Table 3, which shows that the atomic ratio of F/Si is 0.90, and F/C atomic ratio is about 0.38 for the DMS₆₅HFBMA₄₀ diblock copolymer films and the atomic ratio of F/Si is 2.25, and F/C atomic ratio is about 0.72 for the DMS₆₅HFBMA₄₀St₈₃ triblock copolymer films.

4. Conclusions

PDMS-*b*-PHFBMA-*b*-PS triblock copolymers with well-defined structures were successfully synthesized via two-step RAFT polymerization and the polymerization proceeded in a controlled manner in this present work. It provides an applicable approach to prepare novel fluorosilicone block copolymers using a PDMS-macro-RAFT agent with a xanthate group. The results of the WCA measurements indicate that the copolymers are of low surface energy. In addition, the existence of microphase-separation on surfaces primarily consisting of hydrophobic domain from PDMS-*b*-PHFBMA segments are proved by the results of TEM, AFM, and XPS. Moreover, the effects of morphologies and surface compositions of the fluorosilicone copolymers on their surface properties are also investigated. Nevertheless, the surface modification ability of the fluorosilicone copolymers, in other words, the surface energies of polymer films modified by the fluorosilicone copolymers need further investigation.

Acknowledgements

The joint financial supports for this research were provided by the National Natural Science Foundation of China (No. 20406016), Nation Defense Key Laboratory of

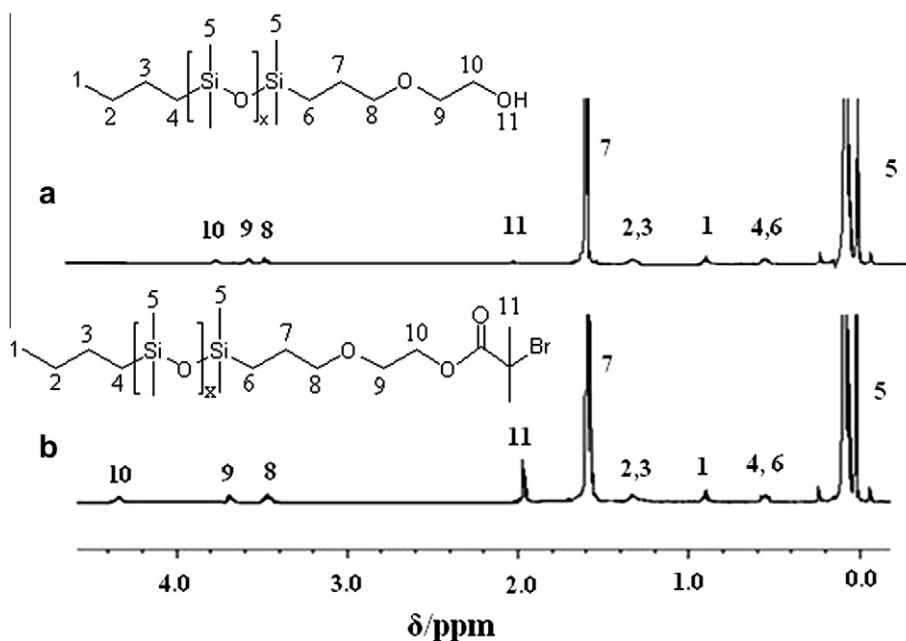


Fig. 7. ¹H NMR spectra ((a) PDMS-OH, (b) PDMS-Br).

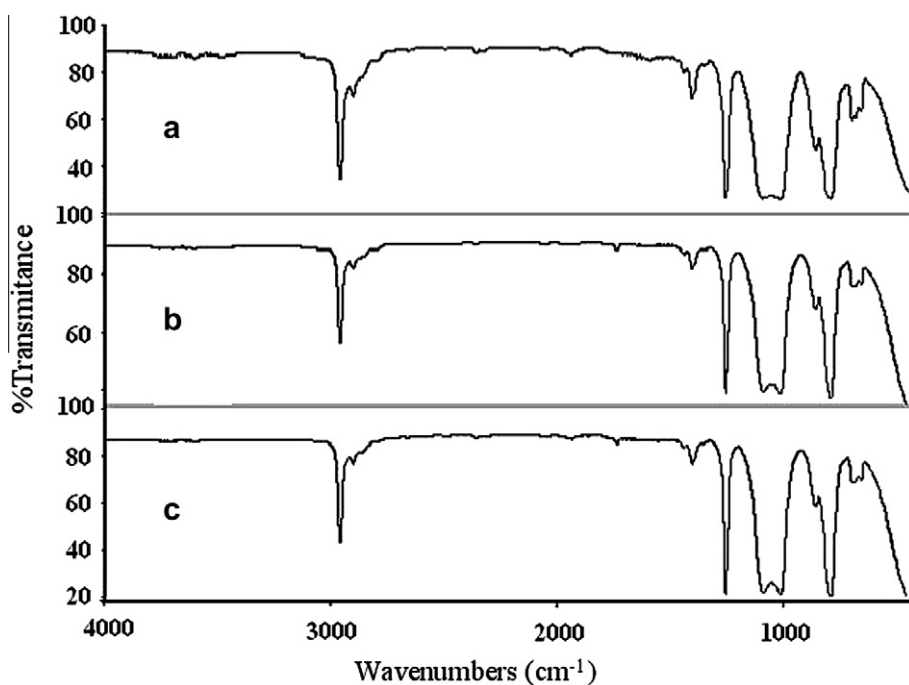


Fig. 8. FT-IR spectra ((a) PDMS-OH, (b) PDMS-Br, (c) PDMS-macro-RAFT agent).

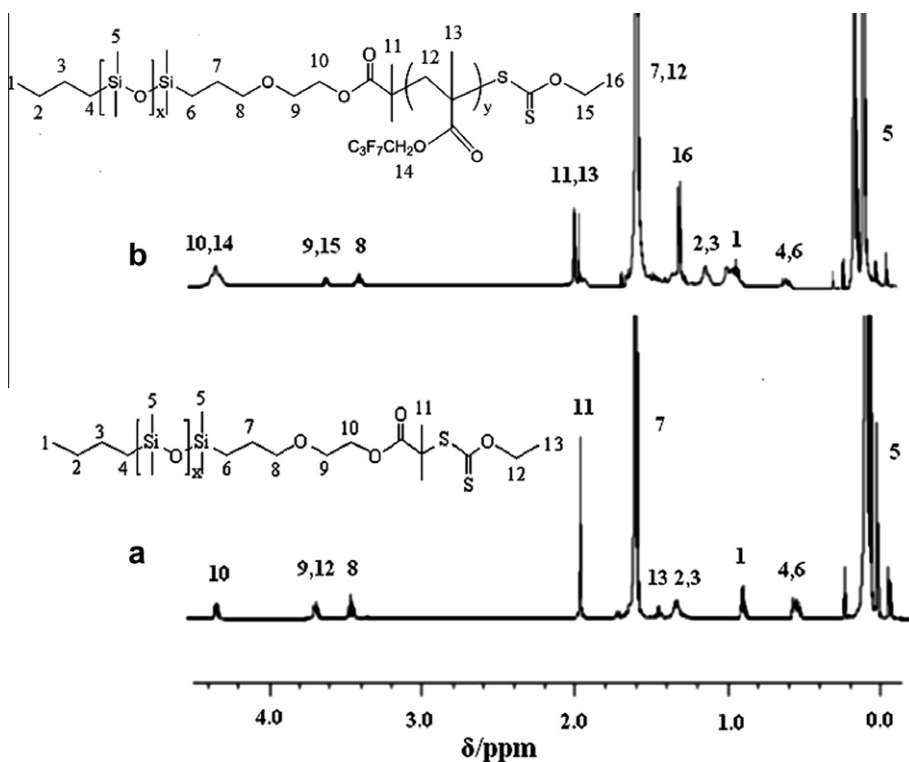


Fig. 9. ^1H NMR spectra ((a) PDMS-macro-RAFT agent, (b) PDMS-*b*-PHFBMA, sample: $\text{DMS}_{65}\text{HFBMA}_{12,6}$).

Ocean Corrosion and Anti-corrosion of China (No. 51449020205QT8703), and Fujian Province Science and Technology Office of China (No. 2005H040). The authors thank Professor Bing-Wei Mao and Yi-Ming Wei (State

Key Laboratory for Physical Chemistry of Solid Surfaces and Department of Chemistry, College of Chemistry and Chemical Engineering, Xiamen University) for AFM analyses.

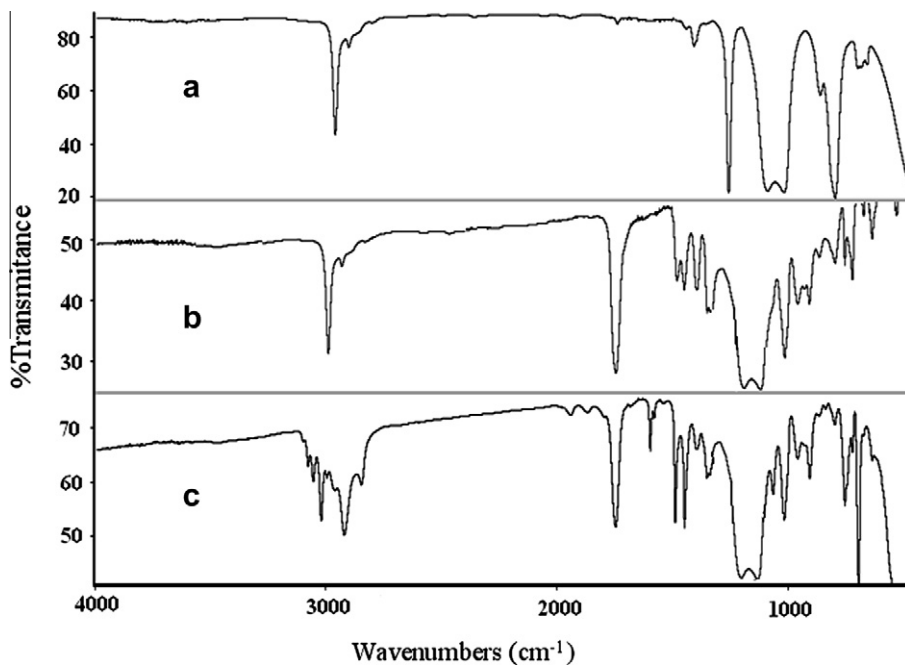


Fig. 10. FT-IR spectra ((a) PDMS-macro-RAFT agent, (b) PDMS-*b*-PHFBMA, (c) PDMS-*b*-PHFBMA-*b*-PS).

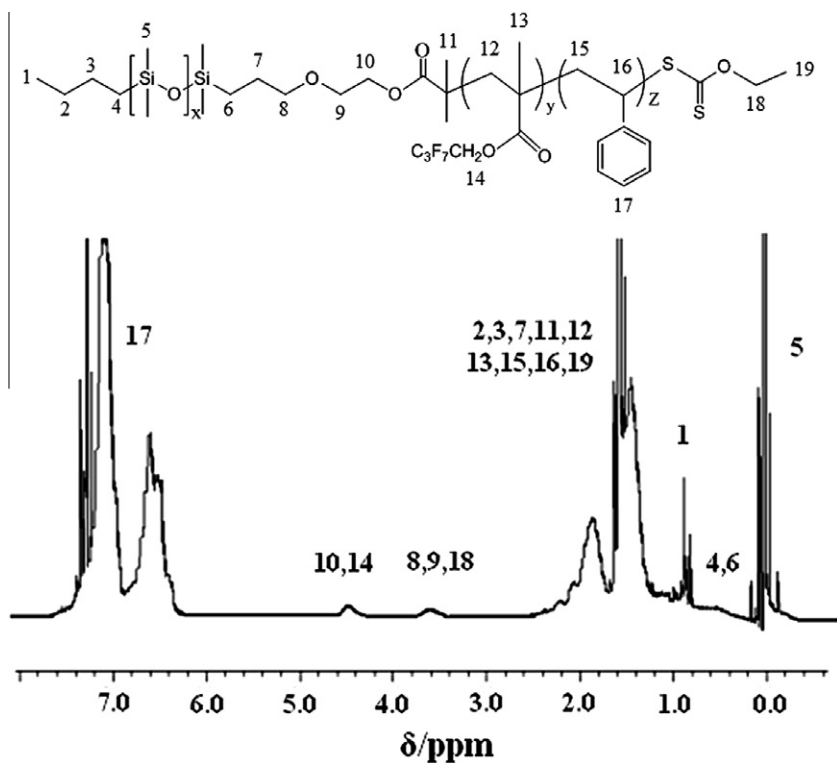


Fig. 11. ^1H NMR spectrum of the PDMS-*b*-PHFBMA-*b*-PS triblock copolymer (sample: DMS₆₅HFBMA₄₀St₈₃).

Appendix A. Experimental procedure for synthesizing PDMS-macro-RAFT agent

All glass instruments and syringes were dried before use. The reaction proceeded under nitrogen atmosphere.

All syringes were degassed three times before use. In a 100 ml round bottom flask, potassium *O*-ethylxanthate (0.1040 g, 0.650 mmol) was dissolved in ethanol (20.0 ml) and PDMS-Br (1.3571 g, 0.260 mmol) was added, and the mixture was stirred for 12 h at room temperature

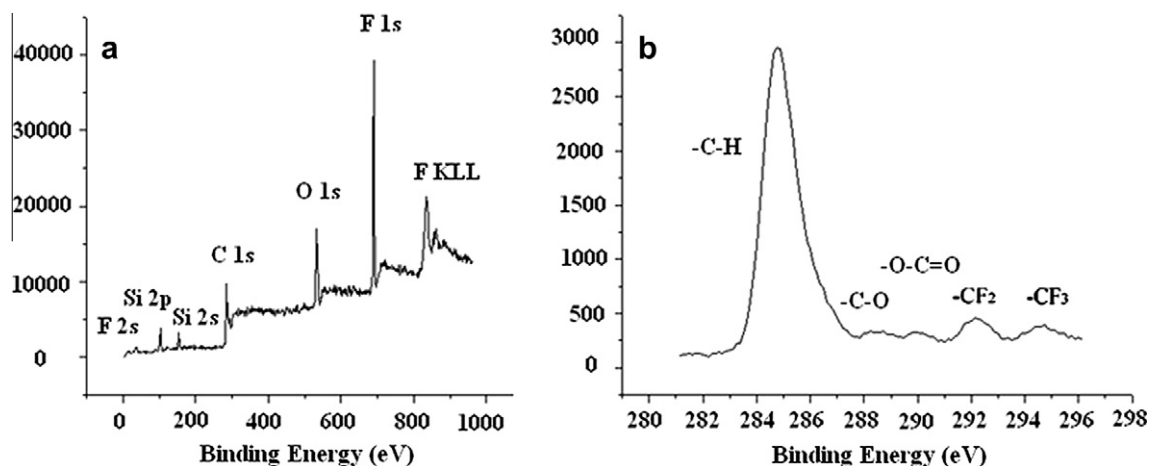


Fig. 12. XPS of DMS₆₅HFBMA₄₀ films ((a) broad scan of the BE spectrum, (b) high-resolution C 1s spectrum).

(Scheme 1). The precipitate was isolated by filtration and washed three times with dichloromethane. The solvent was evaporated to get a pale yellow liquid (yield: 1.1721 g, 80%). The obtained liquid was used as PDMS-macro-RAFT agent for the preparation of diblock copolymers.

Appendix B. Supplementary characterization data of PDMS-Br, PDMS-macro-RAFT agent, and block polymers

Supplementary characterization data of PDMS-Br, PDMS-macro-RAFT agent, and polymer samples are given in Figs. 7–11.

Appendix C. Supplementary XPS data of block polymers

Supplementary XPS data of block polymers are given in Figs. 12 and 13. Fig. 12a is a broad scan of the binding energy (BE) spectrum from 0 to 960 eV for DMS₆₅HFBMA₄₀ diblock copolymer film. It includes four strong and three weak peaks, at approximately 835, 687, 532, 285, 152,

102, and 32 eV, which result from direct photoionization from F KLL, F 1s, O 1s, C 1s, Si 2s, Si 2p, and F 2s core levels, respectively. The high-resolution C 1s spectrum, given in Fig. 12b, of DMS₆₅HFBMA₄₀ diblock copolymer film, exhibits five peaks. The component with BE at 284.7 eV is attributed to the —C—H species. Two peaks at 288.4 and 290.0 eV are assigned to the —C—O— and —O—C=O species of DMS₆₅HFBMA₄₀ diblock copolymer, respectively. The component with BE at 292.2 eV is ascribed to the —CF₂ group and the peak at 294.5 eV results from —CF₃ species. The broad scan of the BE spectrum from 0 to 960 eV for DMS₆₅HFBMA₄₀St₈₃ triblock copolymer film is shown in Fig. 13a. There are also four strong and three weak peaks at approximately 835, 687, 532, 285, 152, 102, and 32 eV that result from direct photoionization from F KLL, F 1s, O 1s, C 1s, Si 2s, Si 2p, and F 2s core levels, respectively. Shown in Fig. 13b is the high-resolution C 1s spectrum of DMS₆₅HFBMA₄₀St₈₃ triblock copolymer film, which exhibits five peaks. The component with BE at 284.7 eV is attributed to the —C—H species. Two peaks at 288.2 and 289.6 eV are attributed to the C—O and —O—C=O species of DMS₆₅HFBMA₄₀St₈₃ triblock copolymer, respectively.

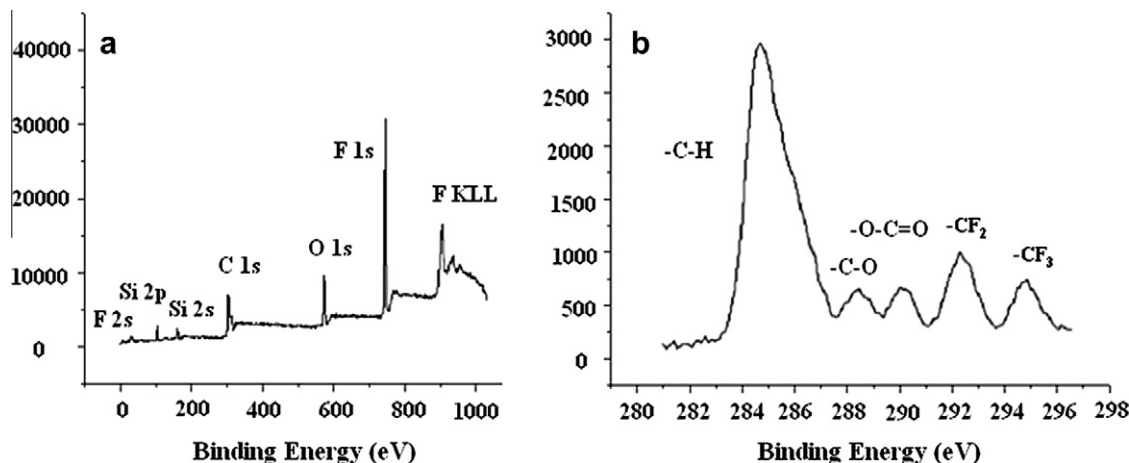


Fig. 13. XPS of DMS₆₅HFBMA₄₀St₈₃ films ((a) broad scan of the BE spectrum, (b) high-resolution C 1s spectrum).

The component with BE at 292.4 eV is ascribed to the —CF_2 group and the peak at 294.8 eV results from —CF_3 species.

References

- [1] Grunlan MA, Mabry JM, Weber WP. Synthesis of fluorinated copoly(carbosiloxane)s by Pt-catalyzed hydrosilylation copolymerization. *Polymer* 2003;44:981–7.
- [2] Ameduri B, Boutevin B. Well-architected fluoropolymers: synthesis, properties and applications. Amsterdam: Elsevier; 2004. 103.
- [3] Ameduri B, Boutevin B, Caporiccio G, Guida-Pietrasanta F, Ratsimihety A. Fluoropolymers. New York: Kluwer Academic Press; 1999. p. 67.
- [4] Guida-Pietrasanta F, Boutevin B, Ratsimihety A. Silicon containing polymers: the science and technology of the synthesis and applications. New York: Kluwer Academic Press; 2001. p. 54.
- [5] Luo ZH, He TY. Synthesis and characterization of poly(dimethylsiloxane)-block-poly(2,2,3,3,4,4,4-heptafluorobutyl methacrylate) diblock copolymers with low surface energy prepared by atom transfer radical polymerization. *React Funct Polym* 2008;68:931–42.
- [6] Arie E, Takazawa T, Yamada S. (Mitsubishi Kasei Corp.). Agricultural synthetic resin covering material. JP 02069538; 1990.
- [7] Ohayashi A, Yamagishi H, Sugiura Y. (Mitsubishi Kasei Vinyl K. K.). Agricultural plasticized polyvinyl chloride-based resin film. JP 03051121; 1991.
- [8] Luo ZH, He TY, Yu HJ, Dai LZ. A novel ABC triblock copolymer with very low surface energy: Poly(dimethylsiloxane)-block-poly(methyl methacrylate)-block-poly(2,2,3,3,4,4,4-heptafluorobutyl methacrylate). *Macromol React Eng* 2008;2:398–406.
- [9] Luo ZH, Yu HJ, Zhang W. Microphase Separation Behavior on the Surfaces of Poly(dimethylsiloxane)-block-poly(2,2,3,3,4,4,4-heptafluorobutyl methacrylate) Diblock Copolymer Coatings. *J Appl Polym Sci* 2008;113:4032–41.
- [10] Hansen NML, Jankova K, Hvilsted S. Fluoropolymer materials and architectures prepared by controlled radical polymerizations. *Eur Polym J* 2007;43:255–93.
- [11] Imae T, Opin C. Fluorinated polymers. *Colloid Interf Sci* 2003;8:307–14.
- [12] Kim DH, Lee SB, Doh KS, Nam YW. Synthesis of urethane craft copolymers with perfluoroalkyl and silicone-containing side chains and their surface properties. *J Appl Polym Sci* 1999;74:2029–38.
- [13] Kim DK, Lee SB. Comparison of surface properties of random, block, and graft copolymers having perfluoroalkyl and silicone-containing side chains. *J Colloid Interface Sci* 2002;247:490–3.
- [14] Kim DK, Lee SB. Surface properties of fluorosilicone copolymers and their surface modification effects on PVC film. *J Colloid Interface Sci* 1998;205:417–22.
- [15] Abdellah L, Dinia MN, Boutevin B, Abadie MJM. Photocalorimetric analysis of the reactivity of crosslinkable polydimethylsiloxanes. *Eur Polym J* 1997;33:869–76.
- [16] Boutevin B, Abdellah L, Dinia M. Synthesis and applications of photocrosslinkable polydimethyl siloxanes—Part III. Synthesis of polysiloxanes with perfluorinated and acrylated urethane linked pendant groups. *Eur Polym J* 1995;31:1127–33.
- [17] Boutevin B, Guida-Pietrasanta F, Ratsimihety A. Synthesis of photocrosslinkable fluorinated polydimethylsiloxanes: Direct introduction of acrylic pendant groups via hydrosilylation. *J Polym Sci A: Polym Chem* 2000;38:3722–8.
- [18] Chen YW, Wang WC, Yu WH, Kang ET, Neoh KG, Ong CK, et al. Ultra-low-kappa materials based on nanoporous fluorinated polyimide with well-defined pores via the RAFT-moderated graft polymerization process. *J Mater Chem* 2004;14:1406–12.
- [19] Eberhardt M, Theato P. RAFT polymerization of pentafluorophenyl methacrylate: Preparation of reactive linear diblock copolymer. *Macromol Rapid Commun* 2005;26:1488–93.
- [20] Inoue Y, Watanabe J, Takai M, Yusa S, Ishihara K. Synthesis of sequence-controlled copolymers from extremely polar and apolar monomers by living radical polymerization and their phase-separated structures. *J Polym Sci A: Polym Chem* 2005;43:6073–83.
- [21] Ma Z, Lacroix-Desmazes P. Synthesis of hydrophilic/ CO_2 -philic poly(ethylene oxide)-b-poly(1,1,2,2-tetrahydroperfluorodecyl acrylate) block copolymers via controlled/living radical polymerizations and their properties in liquid and supercritical CO_2 . *J Polym Sci A: Polym Chem* 2004;42:2405–15.
- [22] Ying L, Yu WH, Kang ET, Neoh KG. Functional and surface-active membranes from poly(vinylidene fluoride)-graft-poly(acrylic acid) prepared via RAFT-mediated graft copolymerization. *Langmuir* 2004;20:6032–40.
- [23] Yu WH, Kang ET, Neoh KG. Controlled grafting of comb copolymer brushes on poly(tetrafluoroethylene) films by surface-initiated living radical polymerizations. *Langmuir* 2005;21:450–6.
- [24] Vana P, Albertin L, Barner L, Davis TP, Barner-Kowollik C. Reversible addition-fragmentation chain-transfer polymerization: Unambiguous end-group assignment via electrospray ionization mass spectrometry. *J Polym Sci A: Polym Chem* 2002;40:4032–7.
- [25] Chiefari J, Mayadunne RTA, Moad CL, Moad G, Rizzardo E, Postma A. Thiocarbonylthio compounds ($\text{S}=\text{C}(\text{Z})\text{S}-\text{R}$) in free radical polymerization with reversible addition-fragmentation chain transfer (RAFT polymerization). Effect of the activating group Z. *Macromolecules* 2003;36:2273–83.
- [26] Li DG, Zhu J, Cheng ZP, Zhang W, Zhu XL. Combination of RAFT and “Click” chemistry techniques to synthesize polymeric europium complexes with selective fluorescence emission. *React Funct Polym* 2009;29:240–5.
- [27] Chen WX, Fan XD, Huang Y, Liu YY, Sun L. Synthesis and characterization of a pentaerythritol-based amphiphilic star block copolymer and its application in controlled drug release. *React Funct Polym* 2009;29:97–104.
- [28] Tong YY, Dong YQ, Du FS, Li ZC. Synthesis of Well-Defined Poly(vinyl acetate)-b-Polystyrene by Combination of ATRP and RAFT Polymerization. *Macromolecules* 2008;41:7339–46.
- [29] Barner-Kowollik C, Davis TP, Heuts JP, Stenzel MH, Vana P, Whittaker M. RAFTing down under: Tales of missing radicals, fancy architectures, and mysterious holes. *J Polym Sci Pol Chem* 2003;41:365.
- [30] Vana P, Quinn JF, Davis TP, Barner-Kowollik C. Recent advances in the kinetics of reversible addition fragmentation chain-transfer polymerization. *Aust J Chem* 2002;55:425–31.
- [31] Zhou D, Zhu XL, Zhu J, Cheng ZP. Preparation and characterization of poly(styrene)/metal composites via reversible addition-fragmentation chain transfer (RAFT) polymerization. *React Funct Polym* 2009;69:55–61.
- [32] Mori H, Iwaya H, Endo T. Controlled synthesis of thermoresponsive polymer via RAFT polymerization of an acrylamide containing L-proline moiety. *React Funct Polym* 2007;67:916–27.
- [33] Perrier S, Takolpuckdee P. Macromolecular design via reversible addition-fragmentation chain transfer (RAFT)/Xanthates (MADIX) polymerization. *Polym Sci A: Polym Chem* 2005;43:5347–93.
- [34] Smulders W, Monteiro MJ. Seeded emulsion polymerization of block copolymer core-shell nanoparticles with controlled particle size and molecular weight distribution using xanthate-based RAFT polymerization. *Macromolecules* 2004;37:4474–83.
- [35] Destarac M, Brochon C, Catala JM, Wilczewska A, Zard SZ. Macromolecular design via the interchange of xanthates (MADIX): Polymerization of styrene with O-ethyl xanthates as controlling agents. *Macromol Chem Phys* 2002;203:2281–5.
- [36] Stenzel MH, Cummins L, Roberts GE, Davis TP, Vana P, Barner-Kowollik C. Xanthate mediated living polymerization of vinyl acetate: A systematic variation in MADIX/RAFT agent structure. *Macromol Chem Phys* 2003;204:1160–8.
- [37] Moad G, Chong YK, Postma A, Rizzardo E, Thang SH. Advances in RAFT polymerization: the synthesis of polymers with defined end-groups. *Polymer* 2005;46:8458–68.
- [38] Wan D, Satoh K, Kamigaito M, Okamoto Y. Xanthate-mediated radical polymerization of N-vinylpyrrolidone in fluoroalcohols for simultaneous control of molecular weight and tacticity. *Macromolecules* 2005;38:10397–405.
- [39] Destarac M, Bzducha W, Taton D, Gauthier-Gillaizeau I, Zard SZ. Direct synthesis of double hydrophilic statistical di- and triblock copolymers comprised of acrylamide and acrylic acid units via the MADIX process. *Macromol Rapid Commun* 2002;23:1049–54.
- [40] Li D, Neumann AW. A reformulation of the equation of state for interfacial tensions. *J Colloid Interf Sci* 1990;137:304–7.
- [41] Li D, Neumann AW. Contact angles on hydrophobic solid surfaces and their interpretation. *J Colloid Interf Sci* 1992;148:190–200.
- [42] Person DV, Fitch JW, Cassidy PE, Kono K, Reddy VS. Polymers from 2,5-difluoroterephthalic acid .1. Polyesters. *React Funct Polym* 1996;30:141–7.
- [43] Sauer BB, Mclean RS, Thomas RR. Tapping mode AFM studies of nano-phases on fluorine-containing polyester coatings and octadecyltrichlorosilane monolayers. *Langmuir* 1998;14:3045–51.
- [44] Brandsch R, Bar G, Whangbo MH. On the factors affecting the contrast of height and phase images in tapping mode atomic force microscopy. *Langmuir* 1997;13:6349–53.